Materials and Manufacturing Processes

Structural and Mechanical Characterization of As-Cast Al-Li-Hf Alloy

Tomás Rangel-Ortiz [ab]; Federico Chávez-Alcalá [a]; E. Curiel-Reyna [b]; Alicia del Real [c]; L. Baños [d]; V. J. Manuel López-Hirata [a]; M. E. Rodríguez [a]

[a] Departamento de Metalurgia y Materiales ESIQIE, Instituto Politécnico Nacional, México, D.F., México
[b] Facultad de Estudios Superiores, Posgrado en Ingeniería, Universidad Nacional Autónoma de México, Cuautitlán, Edo De México, México
[c] Centro de Física Aplicada y Tecnología Avanzada, Departamento de Nanotecnologia, Universidad Nacional Autónoma de México, Campus Juriquilla, Queretaro, Qro, México
[d] Instituto de Investigaciones en Materiales, Ciudad Universitaria, México, D.F., México

PLEASE SCROLL DOWN FOR ARTICLE

Taylor & Francis
Taylor & Francis Group

Structural and Mechanical Characterization of As-Cast Al–Li–Hf Alloy

Tomás Rangel-Ortiz[1,2], Federico Chávez-Alcalá[1], E. Curiel-Reyna[2], Alicia del Real[3], L. Baños[4],
V. J. Manuel López-Hirata[1], and M. E. Rodríguez[1]

[1]Departamento de Metalurgia y Materiales ESIQIE, Instituto Politécnico Nacional, México, D.F. México
[2]Facultad de Estudios Superiores, Posgrado en Ingeniería, Universidad Nacional Autónoma de México, Cuautitlán,
Edo De México, México
[3]Centro de Física Aplicada y Tecnología Avanzada, Departamento de Nanotecnologia, Universidad Nacional Autónoma de México,
Campus Juriquilla, Queretaro, Qro, México
[4]Instituto de Investigaciones en Materiales, Ciudad Universitaria, México, D.F. México

An as-cast Al–Li(2%)–Hf(1%) alloy was structurally and mechanically characterized; X-ray diffraction made it possible to detect the presence of Li and Hf and to determine their effect on aluminum lattice parameter and formation of intermetallic precipitates. The crystalline quality of the Al matrix was influenced by the Li distribution into the Al lattice. The full-width-at-half-maximum was used to determine the crystalline quality of each part of the ingot. The solution of Li in the α-Al matrix decreased the Al lattice parameter and the Hf was found to be present as an intermetallic precipitate, which improve the hardness of the as-cast alloy.

Introduction

Al–Li–Hf alloys offer a unique combination of reduced density, increased elastic modulus, and high strength, compared with those of conventional Al alloys. The combination properties are especially attractive for structural applications in the aerospace industry [1]. The necessities of the development of new metallic materials for applications in the production of pieces with requirements of high quality and low density that can substitute to the traditional alloys and also that present the same or better mechanical proprieties is an important focus in the modern metallurgical industry. The property improvements of Al–Li base alloys have been achieved by allowing the formation of complex precipitates such as $Al_3(Li_xHf_{1-x})$ [2–4]. Al–1.2Li–1Hf alloy has been prepared by using powder metallurgy [5], where they carried out treatments for this alloy and observed a hardening response with good mechanical properties.

Aluminum in combination with lithium is used to form a basic alloy, to which is added one or more metals, in smaller proportion to form a ternary alloy. The third element has a function to increase the toughness of the Al–Li base alloy. It has been also reported that the addition of zirconium or titanium caused the refining of the grain size and increase in mechanical properties; this is also attributed to the corresponding aging treatment [6, 7].

In this work we analyze the structural characteristics of as-cast Al–Li–Hf alloy along the ingot, and determined the Li, and Hf distribution. Additionally the hardness was measured.

Materials and methods

Sample Preparation

A melt of Al–2%Li–1%Hf was prepared as follows: a charge of 970 g of ingot of Al alloy 356 was heated up to 850°C in an electrical resistance furnace. Then, 10 g of flakes of Hf were plunged into the melt, followed by mechanical stirring. Subsequently; the molten alloy was allowed to reach a temperature of 700°C. After this, the same procedure was carried out for lithium addition (23 g). Then, the temperature was increased up to 850°C for 5 min. The alloy melt was cast in rectangular mould wedge-shaped copper. Previously, three thermocouples were mounted at 2.5 cm from the top to the end (see Fig. 1). The copper mould was placed on a copper chill, cooled by a flow of water flow at room temperature, as shown in Fig. 1. The cooling conditions were 2 L min⁻¹ water flow. Three thermocouples of chromel–alumel (K-type) were placed at intervals of 25 mm along the axis from the chill end to the top of the mold. Immediately after pouring the temperature from all the thermocouples was measured using an ERS SR630 thermocouple monitor and data recorder (Stanford Research System, Sunnyvale, CA) using a Microsoft QuickBasic (Redmond, WA) computer program designed for this purpose, thereby obtaining cooling profiles for the experiment [8].

Microhardness Measurements

The Vickers hardness was used to measure the microhardness of the polished samples. The value reported is an average of 30 measurements across the surface of the sample.
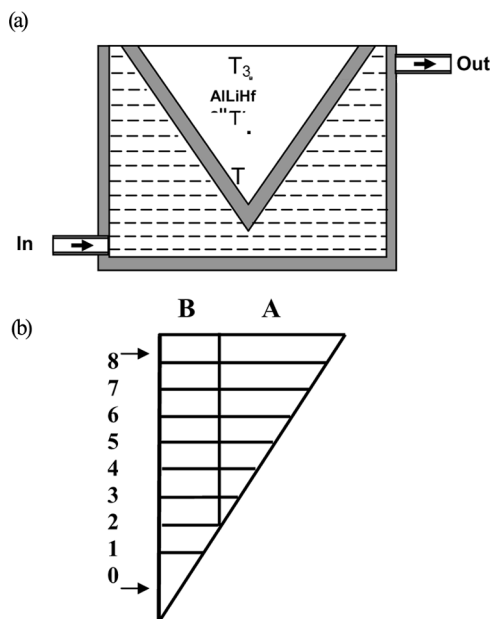
FIGURE 1.—(a) Wedged chapped mold of copper cooling by water. T1 = high cooling zone (tip), T2 = medium cooling zone (central), T3 = lower cooling zone (top). a = 10 cm, b = 11.6 cm. (b) Shows the cut along the longitudinal axis, divided to in two regions A and B that at the same time are divided into sections.

X-Ray Diffraction

The X-Ray diffraction patterns were taken using a Siemmens Crystaloflex 5000 operating at 35 kV, 15 mA with Cu-K$_\alpha$ line. The experimental data to determine the full-width-half-maximum (FWHM) was analyzed using a Dataflex program. The *x*-pattern was used to study the crystalline quality and also shift on the characteristic [111] peak due to the inclusion of lithium [9, 10].

Scanning Electron Microscopy Analysis

The polished samples were examined using a scanning electron microscopy system; Philips XL-30 (The Netherlands) under high vacuum (10^{-5} torr). The samples were examined before any chemical treatment was performed [11].

RESULTS AND DISCUSSIONS

Figure 2 shows the characteristic cooling curves of the Al–Li–Hf, alloy, corresponding to the data collected from three thermocouples located according to Fig. 1(a). The parallel dash lines represent the solid-plus-liquid region. It is possible to observe that the cooling process has different temperature dependence as a function of the thermocouple position. The highest cooling rate was found in the region located at the end of ingot (T1). The intermediate cooling rate was found to be at T2. The top ingot exhibits the slower cooling rate (T3). It is well known that the cooling rate affects the dendrite size and its distribution [12]. Additionally, is possible that these different cooling rates affect the lithium and hafnium distribution along the ingot that could produce changes in the structural characteristics and mechanical properties.
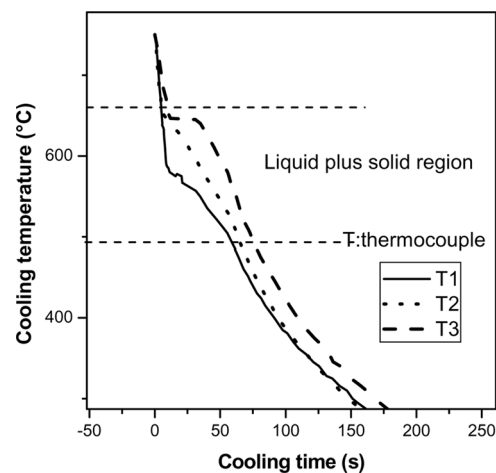

FIGURE 2.—Cooling curves into ingot zones of the Al–Li–Hf alloy, during pouring, solidification and cooling of the same. The superior dotted line, is the solidification beginning zone, the inferior dotted line is the final zone of solidification.

Figures 3(a) and (b) show the X-ray patterns of Al–Li–Hf alloy. This figure shows the characteristic (111) plane of α-Al in the range of 38°C to 39°C in the 2θ scale for a two set of samples labeled as section A and section B (see Fig. 1(b)) which corresponds to 16 samples cut from the ingot. The continuous lines in Figs. 3(a) and (b) correspond to the [111] diffraction peak for Al. According to these figures the chemical composition of each sample is different. These chemical differences could be attributing to different lithium and hafnium distributions and concentration along the ingot and the role of the each one of these elements
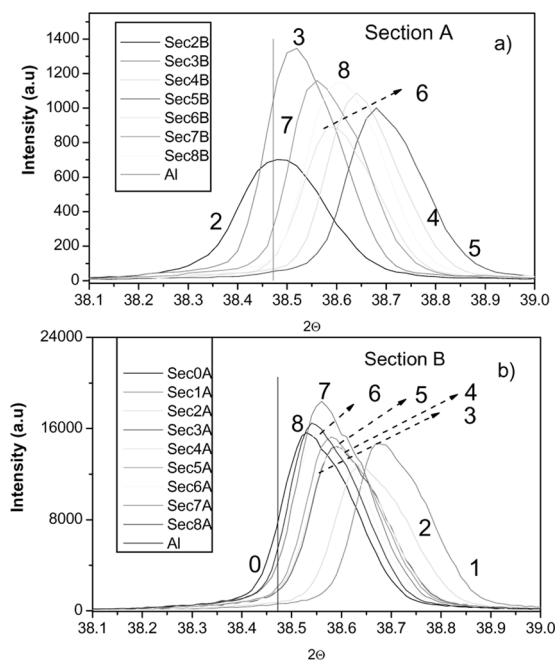

FIGURE 3.—X-ray patterns of Al–Li–Hf alloy. This figure shows the characteristic (111) direction of α-Al in the range of 38° to 39° in the 2θ scale.
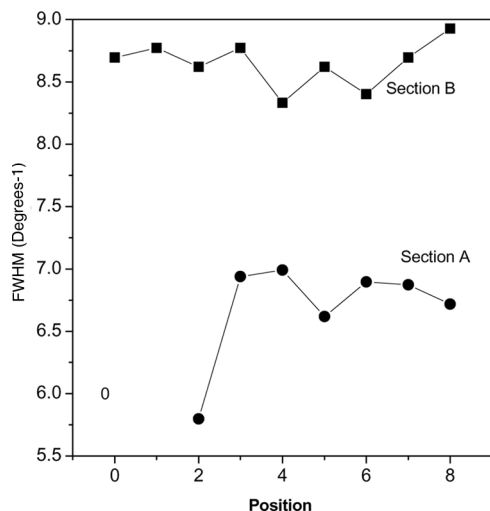
FIGURE 4.—Plot of the $(FWHM)^{-1}$ of the samples as a function of the ingot position for samples from sections A and B.

FIGURE 5.—Al lattice reduction of sections A and B as a function of position.

into the Al structure that could produce important changes in the structural characteristics and mechanical properties.

The fact that there exists a peak shift to high 2θ is indicative of a lattice parameter reduction. This behavior can be associated with the fact that Li is incorporated into the lattice as a substitutional atom; the peak shift does not follow a trend as a function of the sample position, (from of the end to the top). This can be associated with different cooling rates as was showed in Fig. 2. An important point in Figures 3(a) and (b), is related to the changes in the full-width-at-half-medium that according to Rodriguez et al. (2000) [13] and Curiel et al. (2005) [9] is directly associated with the crystalline quality of the Al-rich phase. The FWHM value (FWHM-1) is an indicative parameter to evaluate the relative crystalline quality and also Li interaction with Al-rich matrix.

Figure 4 shows the FWHM value of the samples shown in Fig. 3 (sections A and B). In the central part of the ingot (section B) the crystalline quality is around 20% higher that in section A located in the external part of the ingot. The central part of the ingot is better because the cooling rate is lower, as we can see from Fig. 2. Standard techniques of microcompositional analysis are not presently capable of providing quantitative information about Li composition in the α-Al-rich phase. Energy dispersive spectroscopy (EDS) cannot detect the presence of Li in a sample (Levoy and Vandersande [5]), since the energy of Li–K X-ray is below the delectability limit of available windowless detectors, but according to these results X-ray diffraction is a good tool to study the crystalline quality of the alloy.

Figure 5 shows the 2θ values for the peak of each one of parts in which the ingot was divided as a function of the sample position for samples from sections A and B. As we showed in Fig. 3, the peak shift could be related mainly to the Li entrance into the Al lattice, producing a decrease of lattice parameter [9, 10]. It means that this shift could reflect the distribution into the lattice, and it is a clear that Li is into the Al lattice as a substitutional atom [14]. This figure shows then the Li distributions. According to
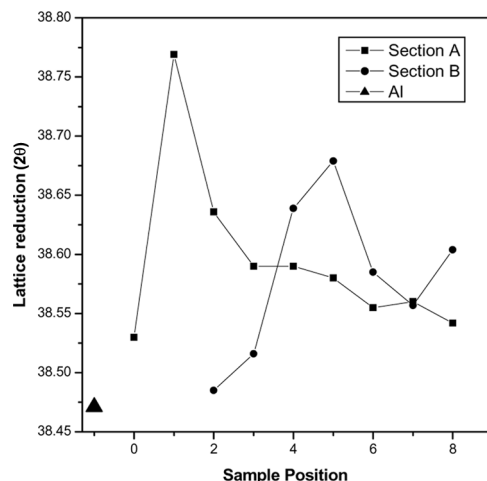
this figure, Li is mainly located at the central part of the ingot. This figure is important because in this way, it is possible to detect directly the content and its distribution. The Li quantification can be solved, by using X-ray powder or in the case of Fig. 2 by correcting the misaligning shift of the peak position for Al (black triangle), taken pure Si as reference.

Figure 6(a) shows the SEM images of the intermetallic precipitate. Its shape is irregular of about 6 µm and composed mainly of Hf (72.42% relative) [15]. By using SEM microanalysis it was not possible to determine the Li concentration in the intermetallic precipitate. Figure 6(b) shows a regular pyramidal precipitate with
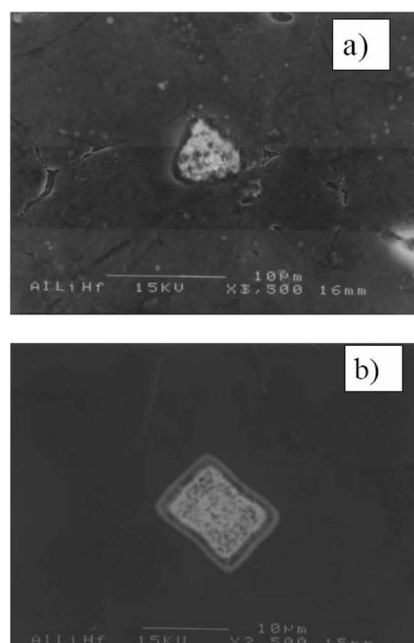
FIGURE 6.—(a) SEM images of an intermetallic Hf precipitate located in sample 6 region B. (b) Corresponds to the intermetallic precipitate located in sample 6 region B.
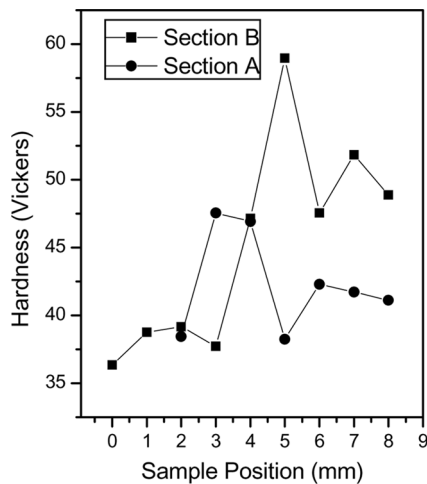
FIGURE 7.—Shows the Vickers hardness numbers of 16 samples from sections A and B as a function of their position.

similar composition (size $12 \times 9\mu m$). The Hf precipitates were found mainly in the central part of ingot; these samples correspond to section B, positions 5 and 6. The main function of these precipitates in the alloy could be to increase the hardness alloy.

Figure 7 shows the Vickers hardnesses of 16 samples from sections A and B (see Fig. 1(b)) as a function of the ingot position. The hardness of this kind of alloy is governed mainly by grain size, the precipitate presence and its distribution. In this case, the samples with the highest hardnesses are located in the central part of the ingot (region B), and, according to Fig. 5, the Li concentration is lower compared to that of region A. SEM images in all samples shower a better distribution of hafnium in the central part of the ingot. These results are in agreement with Fig. 2 because the cooling rate is lower in the central part of the ingot and, as is well known, this fact may improve the hardness, due to the low diffusion of the alloy elements to formed intermetallic precipitates. The size of the intermetallic precipitates was found to be between 6 and $16\mu m$. Levoy and Vandersande [5] studied the Al–1.9Li–1.6Hfd alloy and found that the grains are equiaxed in cross-section, with average size on the order of $2.4\mu m$. No second phase was distinguished in the microstructure of the as-cast material, indicating according to their results that Li and Hf are retained in solution solid in the as-cast materials.

CONCLUSIONS

- Li is incorporated as a substitutional atom in the Al lattice. This result confirms the observations of Donald et al. [14]. This result is confirmed in Fig. 3.
- The crystalline quality of the ingot is higher in the central part (region B) due to the lower cooling rate.
- SEM studies detected the Hf intermetallic precipitates and according to the results shown in Fig. 7 its presence improves the hardness of the alloy.
- According to the foregoing experiments, we have established a new methodology to study the Li distribution along the ingot. By studying the FWHM

of the characteristic [111] peak of Al phase using its shiftment is possible to establish the Li distribution.

REFERENCES

1. Sanders, T.H.; Starke, E. *Alumminum-Lithium Alloys*; TMS-AIME: New York, NY, 1981; 63–67.
2. Norman, A.F.; Tsakiropoulos, P. The microstructure and properties of high pressure gas-atomized Al–Li–Hf alloy powders. Materials Science and Engineering **1991**, *A134*, 1144–1147.
3. Norman, A.F.; Tsakiropoulos, P. The microstructure and properties of rapidly solidified Al–Hf alloys. Material Science Engineering A **1991**, *A134*, 1234–1237.
4. Norman, A.F.; Tsakiropoulos, P. Strengthening mechanisms in powder metallurgy Al–Li–Hf alloys. Metallurgical Transactions A **1989**, *20A*, 228–234.
5. Levoy, N.F.; Vandersande, J.B. Phase transformations in the Al–Li–Hf and Al–Li–Ti systems. Metallurgical Transactions A **1989**, *20A*, 999–1019.
6. Adkins, N.J.E.; Tsakiropoulos, P. Solidification of high pressure gas atomized powders. Part II: Distribution of intermetallic particles in the powder. International Journal Rapid Solidification **1991**, *6*, 101–111.
7. Adkins, N.J.E.; Tsakiropoulos, P. Design of Pm aluminum alloys for applications at elevated temperatures. Part I: The microstructure of high pressure gas atomized powders. Materials Science Technology **1991**, *7*, 334–340.
8. Rangel-Ortiz, T.; Chavez-Alcala, F.; Lopez-Hirata, V.; Frías-Flores, J.; Araujo-Osorio, J.; Dorantes-Rosales, H.J.; Saucedo-Muñoz, M. Microstructure and tensile properties of a continuous-cast Al–Li–Hf alloy. Journal of Materials Processing Technology **2005**, *159*, 164–168.
9. Curiel-Reyna, E.; Herrera, A.; Castaño, V.M.; Rodríguez, M.E. Influence of cooling rate on the structure of heat affected zone after welding a high manganese steel. Materials and Manufacturing Processes **2005**, *20*, 813–822.
10. Pérez-Bueno, J.J.; Rodríguez, M.E.; Zelaya-Ángel, O.; Baquero, R.; González-Hernández, J.; Baños, L.; Fitzpatrick, B.J. Growth and characterization of $Cd_{1-x}Zn_xTe$ crystals with high Zn concentrations. Journal of Crystal Growth **2000**, *209*, 701–708.
11. Adkins, N.J.E.; Norman A.F.; Tsakiropoulos, P. Specimen preparation for Tem studies of rapidly solidified powders. International Journal Rapid Solidification **1991**, *6*, 77–86.
12. Flemings, M.C. *Solidification Processing*; Materials Science and Engineering, McGraw-Hill Series: USA, 1974; 73–78.
13. Rodriguez, M.E.; Zelaya-Angel, O.; Pérez Bueno, J.J.; Jimenez-Sandoval, S.; Tirado, L. Influence of Te inclusions and precipitates on the crystalline and thermal properties of CdTe single crystals. Journal of Crystal Growth **2000**, *213*, 259–266.
14. Donald R. Askeland. *The Science and Engineering of Materials*, 3rd Ed.; PWS Publishing Company, 1998; 254–257.
15. Fahnle M.; Schimmele, L. Atomic defects and diffusion in intermetallic compounds with $D0_3$ structure: an ab-initio study. Z. Metallkunde **2004** *95*, 864–869.